SEARCHING NEW PHYSICS WITH BEAUTY MESONS*

Rusa Mandal, Rahul Sinha

The Institute of Mathematical Sciences, Taramani, Chennai 600113, India
and
Homi Bhabha National Institute, Training School Complex
Anushaktinagar, Mumbai 400094, India

(Received April 20, 2018)

The rare decay $B \to K^* \ell^+ \ell^-$ is an important mode for indirect search of new physics due to the measurement of large number of observables in experiments. Using the most general parametric form of the amplitude in the Standard Model (SM), we probe the physics beyond Standard Model in a theoretically clean approach. The model-independent framework has been implemented in the maximum q^2 limit to highlight strong evidence of right-handed currents, which are absent in the SM. The conclusions derived are free from hadronic corrections. Next, we explain, in terms of a simple and compelling new physics scenario with only two new parameters, the discrepancies between the SM expectations and the data for the neutral-current observables $R_{K^{(*)}}$, as well as the charged-current observables $R(D^{(*)})$ while being consistent with all other data.

DOI:10.5506/APhysPolB.49.1371

1. Introduction

It is a historical fact that several discoveries in particle physics were preceded by indirect evidence through quantum loop contributions. It is for this reason that significant attention is devoted in studying loop processes. The muon magnetic moment is one of the best examples of such a process where precision calculations have been done in order to search for new physics (NP) by comparing the theoretical expectation with experimental observation. It is a testimony to such searches for NP beyond the Standard Model (SM) that both theoretical estimates and experimental observation have reached a precision, where the hadronic effects even for the lepton magnetic moment dominate the discrepancy between theory and observation. Indirect

* Invited talk presented by R. Sinha at the Cracow Epiphany Conference on Advances in Heavy Flavour Physics, Kraków, Poland, January 9–12, 2018.

searches for NP often involve precision measurement of a single quantity that is compared to a theoretical estimate that also needs to be very accurately calculated. Unfortunately, hadronic estimates involve calculation of long-distance QCD effects which cannot easily be done accurately, limiting the scope of such searches. There exist, however, certain decay modes which involve the measurement of several observables that can be related to each other with minimal assumptions and completely calculable QCD contributions within the SM. A well-known example [1–5] of such a process is the semileptonic penguin decay $B \to K^*\ell^+\ell^-$, where ℓ is either the electron or the muon. In Sec. 2, we briefly discuss the results obtained in our recent studies on this mode and refer the reader to Refs. [3, 5] for a detailed description. In Sec. 3, we have identified the minimal modification to the SM in terms of an effective theory that can explain [6] the anomalies in both the charged- and the neutral-current decays of bottom-mesons, a task that has been challenging on account of the seemingly contradictory requirements that the data demands.

2. The rare decay $B \to K^*\ell^+\ell^-$

In this section, first, we briefly discuss the theoretical framework adopted to comprehensively consider almost all possible contributions within the SM for the decay $B \to K^*\ell^+\ell^-$ and then use the model-independent framework to look for a possible NP scenario *i.e.*, right-handed (RH) currents. The most general SM decay amplitude for $B \to K^*\ell^+\ell^-$ reads

$$\begin{aligned} A(B(p) \to K^*(k)\ell^+\ell^-) \;=\; & \frac{G_{\rm F}\alpha}{\sqrt{2}\pi} V_{tb}V_{ts}^* \Big[\Big\{ C_9 \left\langle K^*|\bar{s}\gamma^\mu P_{\rm L} b|\bar{B}\right\rangle \\ & - \frac{2C_7}{q^2} \left\langle K^*|\bar{s} i\sigma^{\mu\nu} q_\nu (m_b P_{\rm R} + m_s P_{\rm L}) b|\bar{B}\right\rangle \\ & - \frac{16\pi^2}{q^2} \sum_{i=\{1-6,8\}} C_i \mathcal{H}_i^\mu \Big\} \\ & \times \bar{\ell}\gamma_\mu \ell + C_{10} \left\langle K^*|\bar{s}\gamma^\mu P_{\rm L} b|\bar{B}\right\rangle \bar{\ell}\gamma_\mu\gamma_5 \ell \Big] , \end{aligned} \tag{1}$$

where, $p = q + k$ and q is the dilepton invariant momentum and C_7, C_9 and C_{10} are the Wilson coefficients. The non-local hadron matrix element $\mathcal{H}_i^\mu$ is given by [7, 8]

$$\mathcal{H}_i^\mu = \langle K^*(k)|\, i \int {\rm d}^4x\, e^{iq\cdot x} T\{ j_{em}^\mu(x), \mathcal{O}_i(0)\} \left\langle \bar{B}(p)\right| \tag{2}$$

which encodes the nonfactorizable contributions arising from charm loop effect. The amplitude written in Eq. (1) is complete and contains all possible effects in SM. Assuring Lorentz and gauge invariance, the hadronic

matrix elements $\langle K^*|\bar{s}\gamma^\mu P_{\rm L} b|\bar{B}(p)\rangle$, $\langle K^*|\bar{s}i\sigma^{\mu\nu}q_\nu P_{\rm R,L} b|\bar{B}(p)\rangle$ and $\mathcal{H}_i^\mu$ can be parametrized in most general form using some "unknown" form factors $X_{0,1,2,3}$, $Y_{1,2,3}$ and $Z_{1,2,3}$, respectively. These from factors are functions of q^2 and no estimations are used for them throughout the work.

The factorizable and non-factorizable corrections [9] up to all order can be absorbed into the redefinition of Wilson coefficients C_9 and C_7 as[1]

$$C_9 \to \widetilde{C}_9^{(j)} = C_9 + \underbrace{\Delta C_9^{(\text{fac})}\left(q^2\right) + \Delta C_9^{(j),(\text{non-fac})}\left(q^2\right)}_{\sim \sum_i C_i \, \mathrm{Z}_j^i/\mathrm{X}_j}, \tag{3}$$

$$\frac{2(m_b+m_s)}{q^2} C_7 \, \mathrm{Y}_j \to \widetilde{\mathrm{Y}}_j = \frac{2(m_b+m_s)}{q^2} C_7 \, \mathrm{Y}_j + \ldots, \tag{4}$$

where $j = 1, 2, 3$ and $\Delta C_9^{(\text{fac})}(q^2)$, $\Delta C_9^{(\text{non-fac})}(q^2)$ are the factorizable and soft gluon non-factorizable contributions respectively and are proportional to the ratio Z_j^i/X_j. Note that due to the introduction of new form factors Z_j, an explicit j dependence is induced in the Wilson coefficients $\widetilde{C}_9^{(j)}$.

We start with the observables as defined in Ref. [3] to be the well-known longitudinal helicity fraction $F_{\rm L}$ and three observables $F_\perp$, A_5, $A_{\rm FB}$ which are related to the CP averaged observables S_3, S_5, $A_{\rm FB}^{\rm LHCb}$ measured by LHCb [10] as follows:

$$F_\perp = \frac{1 - F_{\rm L} + 2S_3}{2}, \qquad A_5 = \frac{3}{4} S_5, \qquad A_{\rm FB} = -A_{\rm FB}^{\rm LHCb}. \tag{5}$$

The observables are functions of transversity amplitudes and in the massless lepton limit, the decay is described by six transversity amplitudes which can be written in the most general form as [3]

$$\mathcal{A}_\lambda^{\rm L,R} = \left(\widetilde{C}_9^\lambda \mp C_{10}\right) \mathcal{F}_\lambda - \widetilde{\mathcal{G}}_\lambda. \tag{6}$$

This parametric form of the SM amplitude includes all short-distance and long-distance effects, factorizable and non-factorizable contributions and resonance contributions up to $\mathcal{O}(G_{\rm F})$. $\mathcal{F}_\lambda$ and $\widetilde{\mathcal{G}}_\lambda$ are combinations of the form factors $X_{0,1,2,3}$ and $Y_{1,2,3}$. The RH current operators O_9' and O_{10}', with respective couplings C_9' and C_{10}', modify the amplitudes as follows:

$$\begin{aligned} \mathcal{A}_\perp^{\rm L,R} &= \left(\left(\widetilde{C}_9^\perp + C_9'\right) \mp \left(C_{10} + C_{10}'\right)\right) \mathcal{F}_\perp - \widetilde{\mathcal{G}}_\perp, \\ \mathcal{A}_{\parallel,0}^{\rm L,R} &= \left(\left(\widetilde{C}_9^{\parallel,0} - C_9'\right) \mp \left(C_{10} - C_{10}'\right)\right) \mathcal{F}_{\parallel,0} - \widetilde{\mathcal{G}}_{\parallel,0}. \end{aligned} \tag{7}$$

[1] Corrections at $q^2 = 0$ are absorbed into C_7 to match it with the coefficient of electromagnetic dipole operator $\mathcal{O}_7$ in $B \to K^*\gamma$ decay and remaining contributions into the coefficient C_9.

With the introduction of notation: $r_\lambda = \mathrm{Re}(\widetilde{\mathcal{G}}_\lambda)/\mathcal{F}_\lambda - \mathrm{Re}(\widetilde{C}_9^\lambda)$, $\xi = C'_{10}/C_{10}$, and $\xi' = C'_9/C_{10}$, we construct the following variables:

$$R_\perp = \left(\frac{r_\perp}{C_{10}} - \xi'\right) \Big/ (1+\xi)\,, \qquad R_{\parallel,0} = \left(\frac{r_{\parallel,0}}{C_{10}} + \xi'\right) \Big/ (1-\xi)\,. \tag{8}$$

At low recoil energy of K^* meson, only three independent form factors describe the whole $B \to K^*\ell^+\ell^-$ decay and there exists a relation among the form factors at leading order in $1/m_B$ expansion given by [8, 11], $\widetilde{\mathcal{G}}_\parallel/\mathcal{F}_\parallel = \widetilde{\mathcal{G}}_\perp/\mathcal{F}_\perp = \widetilde{\mathcal{G}}_0/\mathcal{F}_0 = -\kappa\, 2m_b m_B C_7/q^2$, where $\kappa \approx 1$. Hence, at the maximum point in q^2 *i.e.*, the kinematic endpoint $q^2_{\rm max}$, one defines r such that $r_0 = r_\parallel = r_\perp \equiv r$. Therefore, Eq. (8) implies that in the presence of RH currents, one should expect $R_0 = R_\parallel \neq R_\perp$ at $q^2 = q^2_{\rm max}$ without any approximation. Interestingly, this relation is unaltered by non-factorizable and resonance contributions [12] at this kinematic endpoint. To test the relation among R_λs in light of LHCb data, first defining $\delta \equiv q^2_{\rm max} - q^2$, we expand the observables $F_{\rm L}$, $F_\perp$, $A_{\rm FB}$ and A_5 around $q^2_{\rm max}$ as follows:

$$\begin{aligned} F_{\rm L} &= \tfrac{1}{3} + F_{\rm L}^{(1)}\delta + F_{\rm L}^{(2)}\delta^2 + F_{\rm L}^{(3)}\delta^3\,, & F_\perp &= F_\perp^{(1)}\delta + F_\perp^{(2)}\delta^2 + F_\perp^{(3)}\delta^3\,, \\ A_{\rm FB} &= A_{\rm FB}^{(1)}\delta^{\frac{1}{2}} + A_{\rm FB}^{(2)}\delta^{\frac{3}{2}} + A_{\rm FB}^{(3)}\delta^{\frac{5}{2}}\,, & A_5 &= A_5^{(1)}\delta^{\frac{1}{2}} + A_5^{(2)}\delta^{\frac{3}{2}} + A_5^{(3)}\delta^{\frac{5}{2}}\,. \end{aligned} \tag{9}$$

The zeroth order coefficients of the observable expansions are assumed from the constraints arising from Lorentz invariance and decay kinematics derived in Ref. [12], whereas all the higher order coefficients are extracted by fitting the polynomials with 14 bin LHCb data as shown in Fig. 1.

The limiting analytic expressions for R_λ at $q^2 = q^2_{\rm max}$ are

$$R_\perp\left(q^2_{\rm max}\right) = \frac{\omega_2 - \omega_1}{\omega_2\sqrt{\omega_1 - 1}}\,, \qquad R_\parallel\left(q^2_{\rm max}\right) = \frac{\sqrt{\omega_1 - 1}}{\omega_2 - 1} = R_0\left(q^2_{\rm max}\right)\,, \tag{10}$$

$$\text{where} \quad \omega_1 = \frac{3F_\perp^{(1)}}{2A_{\rm FB}^{(1)\,2}} \quad \text{and} \quad \omega_2 = \frac{4\left(2A_5^{(2)} - A_{\rm FB}^{(2)}\right)}{3\,A_{\rm FB}^{(1)}\left(3F_{\rm L}^{(1)} + F_\perp^{(1)}\right)}\,. \tag{11}$$

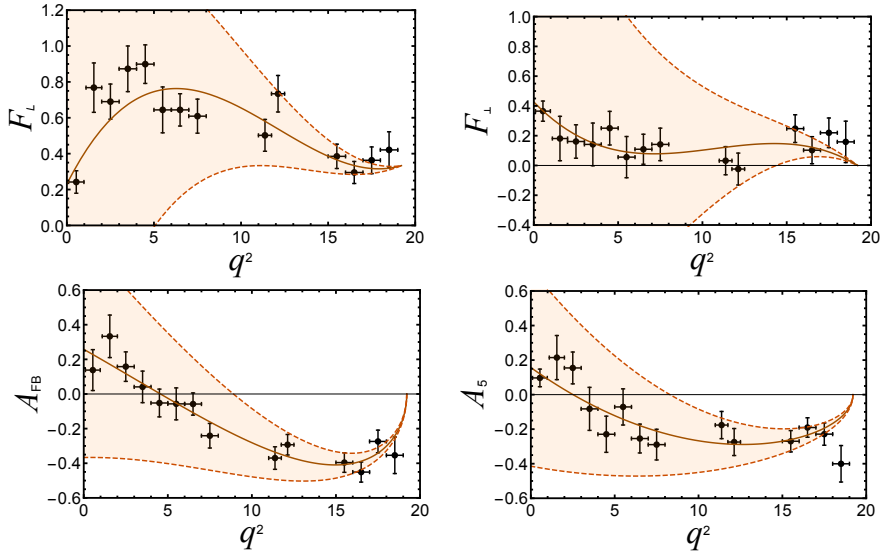

Fig. 1. (Color online) An analytic fit to 14-bin LHCb data using the Taylor expansion at $q^2_{\rm max}$ for the observables $F_{\rm L}$, $F_\perp$, $A_{\rm FB}$ and A_5 are shown as the solid/brown curves. The $\pm 1\sigma$ error bands are indicated by the light gray/brown shaded regions, derived including correlation among all observables. The points with the black error bars are LHCb 14-bin measurements [10].

It can be seen that ω_1, ω_2 contain coefficients which are extracted completely from data and their estimates using LHCb measurements are: $\omega_1 = 1.10 \pm 0.30$ (1.03 ± 0.34) and $\omega_2 = -4.19 \pm 10.48$ (-4.04 ± 10.12), where the first values are determined using $A^{(1)}_{\rm FB}$ and the values in the round brackets use $2A^{(1)}_5$. The variables R_λs can be estimated using data only and the allowed region is shown in gray bands in Fig. 2. A significant deviation is seen from a slope of 45° line (black/red line) which denotes $R_\perp = R_\parallel = R_0$ and thus hints toward the presence of RH currents without *using any estimate of hadronic contributions.*

To quantify the RH couplings, we use Eq. (8) and the results are shown in Fig. 3. The left panel uses the SM estimate of parameter r/C_{10} [11] and the SM prediction for C'_{10}/C_{10} and C'_9/C_{10} (the origin) is at more than 5σ confidence level. We have performed another analysis where the input r/C_{10} is considered as nuisance parameter and the result is shown in the right most panel of Fig. 3. It can be seen that the uncertainties in fitted parameters C'_{10}/C_{10} and C'_9/C_{10} have increased due to the variation of r/C_{10} and the SM prediction still remains on a 3σ level contour providing evidence of RH currents.

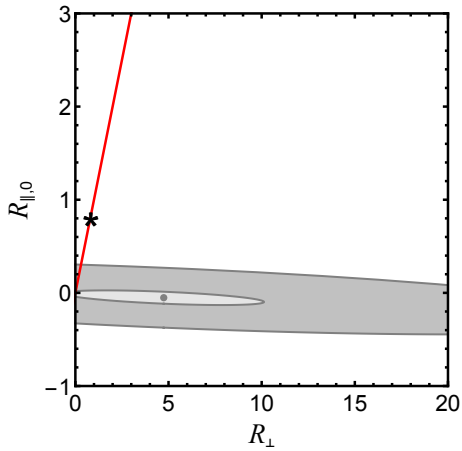

Fig. 2. (Color online) Allowed regions in $R_\perp$–$R_{\|,0}$ plane are shown in light and dark gray bands at 1σ and 5σ confidence level, respectively. The black/red straight line corresponds to the case $R_\perp = R_{\|,0}$ *i.e.* the absence of RH couplings. The SM prediction denoting by the black star corresponds to $R_\perp = R_0 = R_\| = 0.84$.

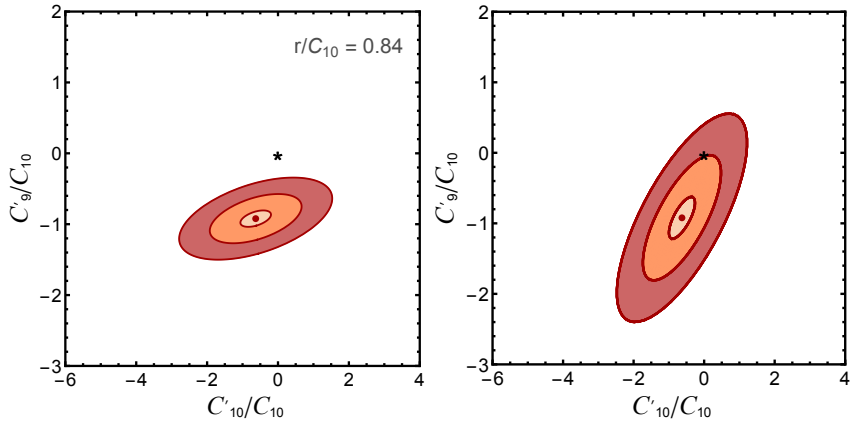

Fig. 3. (Color online) (Left panel) In C'_{10}/C_{10}–C'_9/C_{10} plane, the light gray/yellow, gray/orange and dark gray/red regions correspond to 1σ, 3σ and 5σ significance level, respectively, where SM input for r/C_{10} [11] is used. The best fit values of C'_{10}/C_{10} and C'_9/C_{10}, with $\pm 1\sigma$ errors are -0.63 ± 0.43 and -0.92 ± 0.10, respectively. (Right panel) The same color code as the left panel figure. The input r/C_{10} is varied as a nuisance parameter and hence the obtained uncertainties in C'_{10}/C_{10} and C'_9/C_{10} are increased. The SM predictions for both the plots are indicated by the stars. Strong evidence of RH current is pronounced from the plots.

2.1. Some sanity checks

2.1.1. Resonance effects

Resonances can alter the results that are obtained using a polynomial fit to the observables in Eq. (9), where it is assumed that resonances are absent. To study the systematics due to resonances, we assume observables calculated using theoretical estimates of form factors (LCSR [13] for $q^2 \leq 15$ GeV^2 and Lattice QCD [14] for $q^2 \geq 15$ GeV^2 region) and Wilson coefficients. Following the parametrization from Ref. [15], we include the $J/\psi(1S)$, $\psi(2S)$, $\psi(3770)$, $\psi(4040)$, $\psi(4160)$ and $\psi(4415)$ resonances in our study. The procedure uses the function $g(m_c, q^2)$, in Wilson coefficient $C_9^{\rm eff}$, which includes the cross-section ratio $R^{c\bar{c}}_{\rm had}(q^2) = R^{c\bar{c}}_{\rm cont}(q^2) + R^{c\bar{c}}_{\rm res}(q^2)$, where the resonance effects are incorporated as

$$R^{c\bar{c}}_{\rm res}\left(q^2\right) = N_{\rm r} \sum_{V=J/\psi,\psi'\ldots} \frac{9\,q^2}{\alpha} \frac{{\rm BR}(V \to \ell^+\ell^-)\Gamma^V_{\rm tot}\Gamma^V_{\rm had}}{\left(q^2 - m_V^2\right)^2 + m_V^2\Gamma^{V2}_{\rm tot}} e^{i\delta_V} \,. \tag{12}$$

Here, $\Gamma^V_{\rm tot}$ is the total width of the vector meson V, δ_V is an arbitrary relative strong phase associated with each of the resonances and $N_{\rm r}$ is a normalization factor that fixes the size of the resonance contributions compared to the non-resonant background. A random simulation has been done by varying each resonance phases δ_V and a sample of plots for different observables are given in link [16] as movies. It can be seen from the plots that when resonances are included, $A_{\rm FB}$ and A_5 always decrease in magnitude for the 15 GeV$^2 \leq q^2 \leq 19$ GeV^2 region. Hence, if the effect of resonances could somehow be removed from the data, the values of $A_{\rm FB}$ and A_5 would be larger in magnitude which, in turn, will decrease the value of observable ω_1 compared to the values obtained from fits to experimental data in which resonances are automatically present. As the current obtained values of ω_1 from data are already close to unity, any further reduction will force ω_1 into the un-physical domain and increase the significance of deviation from the SM.

2.1.2. Polynomial fit convergence

In this section, we study the systematics of the fits to coefficients $A^{(1)}_{\rm FB}$, $A^{(2)}_{\rm FB}$, $F^{(1)}_{\rm L}$, $A^{(1)}_5$, $A^{(2)}_5$ and $F^{(1)}_\perp$, which appear in the expressions of ω_1 and ω_2 given in Eq. (11). By varying the order of the polynomial fitted from 2 to 4, and also the number of bins from the last 4 to 14 bins, each extracted coefficients is shown in Fig. 4. We find that all the fitted coefficients show a good degree of convergence even when larger number of bins are added. The values obtained for the coefficients are consistent within $\pm 1\sigma$ regions apart

from some small mismatches in $F_\perp^{(1)}$ and $A_5^{(1)}$. We choose as a benchmark the third order polynomial fit to all 14 bins and to validate this choice, we also perform an identical fit for observables generated using form factor values [13, 14] and the results are shown in Fig. 5. The fits to SM observables are satisfactory for the entire q^2 region.

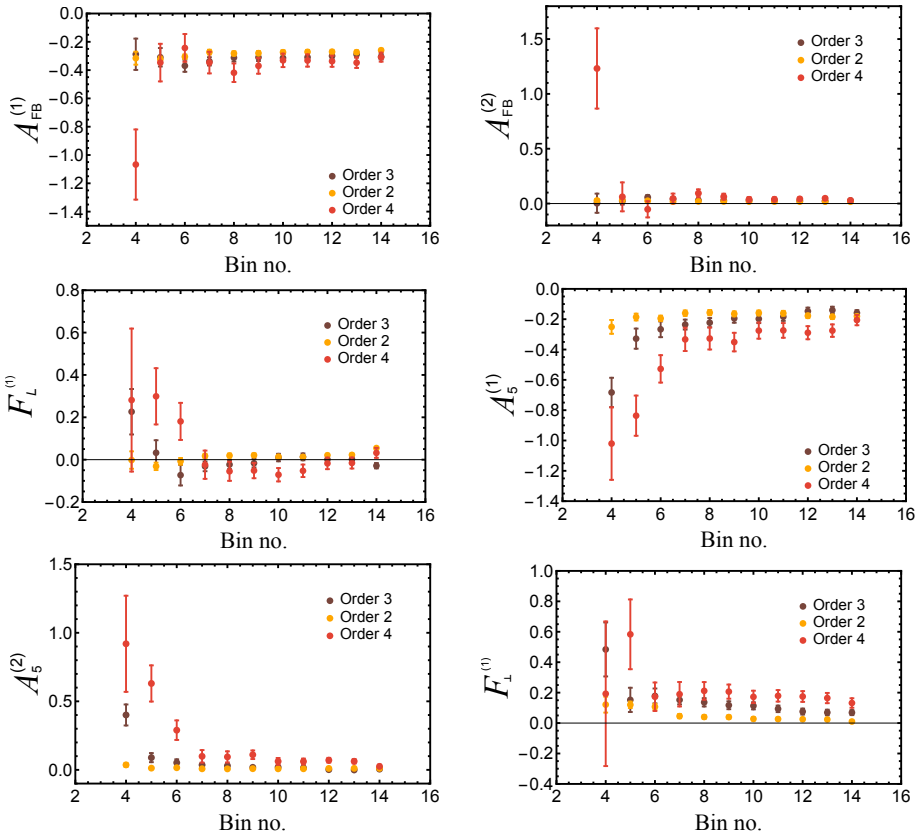

Fig. 4. (Color online) Systematic study of the coefficients of observables with the variation of polynomial order and the number of bins used for the fit. The color code for the different orders of the fitted polynomial is depicted in the panel. The x-axis denotes the number of bins used for the fit from last 4 to 14 bins. Coefficient values show good convergence within the $\pm 1\sigma$ error bars except for few bins in the $F_\perp^{(1)}$ and $A_5^{(1)}$ distributions. The 4-bin order 4 polynomial fit shows disagreement which is expected.

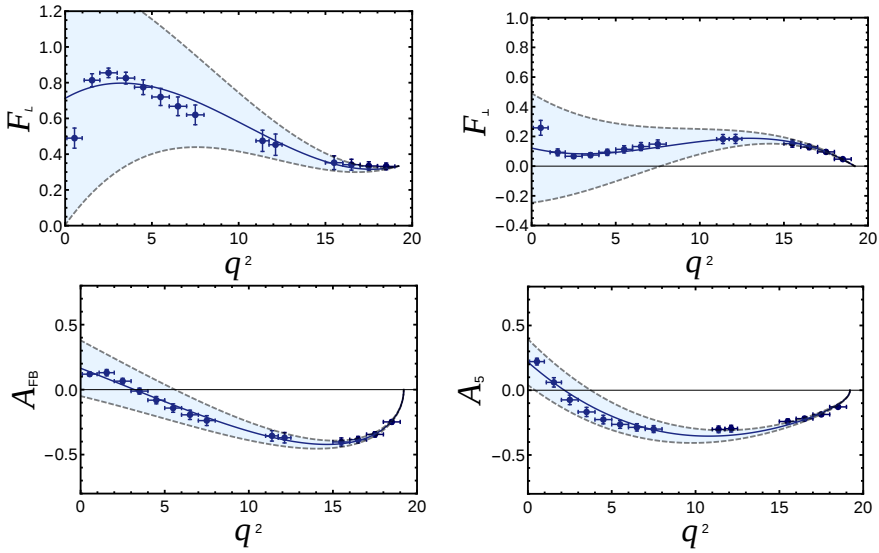

Fig. 5. (Color online) Fits with third order polynomials to the theoretical SM observables, generated using LCSR form factors for $q^2 \leq 15$ GeV^2 [13] and Lattice QCD form factors for $q^2 \geq 15$ GeV^2 [14]. The gray/blue error bars are bin integrated SM estimates and the solid black/blue curve with the shaded region represents the best fit polynomial with $\pm 1\sigma$ errors. The fits nicely explain the SM observables including the zero-crossing of asymmetries $A_{\rm FB}$ and A_5.

3. Lepton flavor non-universality

The intriguing discrepancies between the SM expectations and the data for the neutral-current observables R_K and R_{K^*}, as well as the charged-current observables $R(D)$ and $R(D^*)$ have drawn great attentions. With the ratios of partial widths, these observables are particularly clean probes of physics beyond the SM. The ratios for charged-current are defined as

$$R\left(D^{(*)}\right) \equiv \frac{\mathrm{BR}\left(B \to D^{(*)}\tau\nu\right)}{\mathrm{BR}\left(B \to D^{(*)}\ell\nu\right)}, \qquad \ell \in \{e, \mu\} \tag{13}$$

and analogous ratios for the neutral-current sector

$$R_{K^{(*)}} \equiv \frac{\mathrm{BR}\left(B \to K^{(*)}\mu\mu\right)}{\mathrm{BR}\left(B \to K^{(*)}ee\right)}. \tag{14}$$

The measurements for $R(D)$ and $R(D^*)$ [17] show $\sim 2.3\sigma$ and $\sim 3.4\sigma$ discrepancy respectively. The data on R_K [18] and R_{K^*} [19], on the other hand, lie systematically below the SM expectations with significance of $\sim 2\sigma$.

In this section, we show that an simultaneous explanation can be achieved in an effective theory with only two unknown parameters. We propose a model involving two four-fermi operators in terms of the second and third generation (weak-eigenstate) fields [6]

$$\mathcal{H}^{\rm NP} = A_1 \left(\bar{Q}_{2\rm L}\gamma_\mu L_{3\rm L}\right)\left(\bar{L}_{3\rm L}\gamma^\mu Q_{3\rm L}\right) + A_2 \left(\bar{Q}_{2\rm L}\gamma_\mu Q_{3\rm L}\right)\left(\bar{\tau}_{\rm R}\gamma^\mu \tau_{\rm R}\right) , \qquad (15)$$

where we demand $A_2 = A_1$. This operator contributes to $R(D^{(*)})$, however, the contribution to $R_{K^{(*)}}$ can be generated by the simplest of field rotations for the left-handed leptons from the unprimed (flavor) to the primed (mass) basis, namely,

$$\tau = \cos\theta\,\tau' + \sin\theta\,\mu' , \qquad \nu_\tau = \cos\theta\,\nu'_\tau + \sin\theta\,\nu'_\mu . \qquad (16)$$

A chi-square fit to observables $R(D)$, $R(D^*)$, R_K, $R^{\rm low}_{K^*}$, $R^{\rm cntr}_{K^*}$, $\mathrm{dBR}(B_{\rm s} \to \phi\mu\mu)/\mathrm{d}m^2_{\mu\mu}$ (in the bin $m^2_{\mu\mu} \in [1 : 6]\,\mathrm{GeV}^2$) with best fit points $A_1(= A_2) = -2.92\,\mathrm{TeV}^{-2}$, $\sin\theta = \pm 0.022$ provides a reasonable explanation to all observables except for $R^{\rm low}_{K^*}$, while being consistent with all data. We illustrate, in Fig. 6, that allowing a 20% breaking of the relation as given by $A_2 = 4A_1/5$, the fit can be improved remarkably. The χ^2/d.o.f. is equal to 2 in the region allowed by $B^+ \to K^+\mu^-\tau^+$ upper limit. The origin of this split between the A_i can be attributed as the difference to the quantum numbers of the leptonic fields under an as yet unidentified gauge symmetry, with the attendant anomaly cancellation being effected by either invoking heavier fermionic fields or through other means.

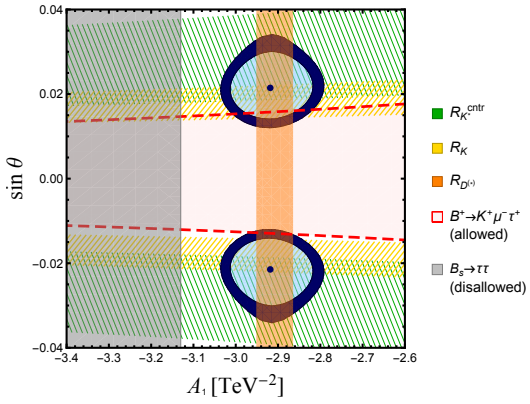

Fig. 6. The fit for $A_2 = 4A_1/5$, with the bands around the best-fit points corresponding to 95% and 99% C.L. Also shown are the 1σ bands from $R_{K^{(*)}}$ and $R(D)$, and the 95% upper limits from $B_s \to \tau\tau$ and $B^+ \to K^+\mu^-\tau^+$.

4. Summary

— A formalism has been developed to incorporate almost all possible effects within the SM. The approach we have adopted in our work differs from other approaches [20] in literature as we have no or minimal dependency on hadronic uncertainties.

— A strong evidence of RH currents is found where the conclusions are derived at endpoint limit.

— The detailed study of resonance effects strengthen the conclusion derived here.

— A systematic study, by varying the polynomial order (Eq. (9)) and the number of bins used to fit the polynomials, shows a very good convergence for fit coefficients.

— The finite width effect of K^* meson has also been considered where the position of the kinematic endpoint $q^2_{\rm max}$ is varied over a range considering width of $K^* \sim 50\,\text{MeV}$. Using a weighted average over the Breit–Wigner shape for K^* meson, the ω_1 and ω_2 values are found well within the $\pm 1\sigma$ uncertainties of the results obtained without the width effect.

— In the later part of this article, in terms of effective operators we show a possible explanation to all the lepton non-universal anomalies seen in B decays.

— The model has only two new parameters and predicts some interesting signatures both in the context of B decays, especially in $B_s \to \tau\tau$, $B \to K^{(*)}\mu\tau$ modes, as well as in high-energy collisions.

— We conclude that it is a very interesting era for B physics and there is need for more data from experiments to confirm/falsify the presence of the NP scenarios presented here.

We would like to thank D. Choudhury, A. Karan, A. Kundu and A.K. Nayak for collaboration on different parts of the work presented in the paper.

REFERENCES

[1] F. Kruger, L.M. Sehgal, N. Sinha, R. Sinha, *Phys. Rev. D* **61**, 114028 (2000) [arXiv:hep-ph/9907386].

[2] D. Das, R. Sinha, *Phys. Rev. D* **86**, 056006 (2012) [arXiv:1205.1438 [hep-ph]].

[3] R. Mandal, R. Sinha, D. Das, *Phys. Rev. D* **90**, 096006 (2014).

[4] R. Mandal, R. Sinha, *Phys. Rev. D* **95**, 014026 (2017).

[5] A. Karan *et al.*, *Phys. Rev. D* **95**, 014026 (2017); **95**, 114006 (2017) [arXiv:1603.04355 [hep-ph]].

[6] D. Choudhury, A. Kundu, R. Mandal, R. Sinha, *Phys. Rev. Lett.* **119**, 151801 (2017) [arXiv:1706.08437 [hep-ph]].

[7] A. Khodjamirian, T. Mannel, A.A. Pivovarov, Y.-M. Wang, *J. High Energy Phys.* **1009**, 089 (2010) [arXiv:1006.4945 [hep-ph]].

[8] B. Grinstein, D. Prijol, *Phys. Rev. D* **70**, 114005 (2004).

[9] M. Beneke, T. Feldmann, D. Seidel, *Nucl. Phys. B* **612**, 25 (2001) [arXiv:hep-ph/0106067].

[10] R. Aaij *et al.* [LHCb Collaboration], *J. High Energy Phys.* **1602**, 104 (2016).

[11] C. Bobeth, G. Hiller, D. van Dyk, *J. High Energy Phys.* **1007**, 098 (2010).

[12] G. Hiller, R. Zwicky, *J. High Energy Phys.* **1403**, 042 (2014).

[13] A. Bharucha, D.M. Straub, R. Zwicky, *J. High Energy Phys.* **1608**, 098 (2016).

[14] R.R. Horgan, Z. Liu, S. Meinel, M. Wingate, *Phys. Rev. Lett.* **112**, 212003 (2014).

[15] F. Kruger, L.M. Sehgal, *Phys. Lett. B* **380**, 199 (1996) [arXiv:hep-ph/9603237].

[16] http://www.imsc.res.in/∼abinashkn/arXiv

[17] Y. Amhis *et al.* [HFLAV Collaboration], *Eur. Phys. J. C* **77**, 895 (2017) [arXiv:1612.07233 [hep-ex]].

[18] R. Aaij *et al.* [LHCb Collaboration], *Phys. Rev. Lett.* **113**, 151601 (2014) [arXiv:1406.6482 [hep-ex]].

[19] R. Aaij *et al.* [LHCb Collaboration], *J. High Energy Phys.* **1708**, 055 (2017) [arXiv:1705.05802 [hep-ex]].

[20] W. Altmannshofer, D.M. Straub, *Eur. Phys. J. C* **75**, 382 (2015); M. Ciuchini *et al.*, *J. High Energy Phys.* **1606**, 116 (2016); S. Jäger, J. Martin Camalich, *Phys. Rev. D* **93**, 014028 (2016); S. Descotes-Genon, L. Hofer, J. Matias, J. Virto, *J. High Energy Phys.* **1606**, 092 (2016).